Environmental Science and Pollution Research (2023) 30:44566–44577
https://doi.org/10.1007/s11356-023-25383-0

RESEARCH ARTICLE

Biosynthesized silver nanoparticles have anticoccidial and jejunum-protective effects in mice infected with *Eimeria papillata*

Mohamed A. Dkhil[1,2] · Felwa A. Thagfan[3] · Mostafa Y. Morad[1] · Esam M. Al-Shaebi[4] · Sherif Elshanat[5] · Amira A. Bauomy[6] · Murad Mubaraki[7] · Taghreed A. Hafiz[7] · Saleh Al-Quraishy[4] · Rewaida Abdel-Gaber[4]

Received: 7 June 2022 / Accepted: 13 January 2023 / Published online: 25 January 2023

Abstract

Eimeriosis, an infection with *Eimeria* spp. that affects poultry, causes huge economic losses. Silver nanoparticles (AgNPs) have antibacterial and antifungal properties, but their action against *Eimeria* infection has not yet been elucidated. This study demonstrates the action of AgNPs in the treatment of mice infected with *Eimeria papillata*. AgNPs were prepared from *Zingiber officinale* rhizomes. Phytochemical screening by gas chromatography–mass spectrometry analysis (GC–MS) was used to detect active compounds. Mice were divided into five groups: uninfected mice, uninfected mice that were administered AgNPs, untreated mice infected with 10^3 sporulated oocysts of *E. papillata*, infected mice treated with AgNPs, and infected mice treated with amprolium. Characterization of the samples showed the AgNPs to have nanoscale sizes and aspherical shape. Phytochemical screening by GC–MS demonstrated the presence of 38 phytochemical compounds in the extract of *Z. officinale*. Mice infected with *E. papillata*-sporulated oocysts were observed to have many histopathological damages in the jejuna, including a decrease in the goblet cell numbers affecting the jejunal mucosa. Additionally, an increased oocyst output was also observed. The treatment of infected mice with AgNPs resulted in the improvement of the jejunal mucosa, increase in the number of goblet cell, and decrease in the number of meronts, gamonts, and developing oocysts in the jejuna. Moreover, AgNPs also led to decreased oocyst shedding in feces. The results revealed AgNPs to have an anticoccidial effect in the jejunum of *E. papillata*-infected mice and, thus, could be a potential treatment for eimeriosis.

Keywords Coccidiosis · AgNPs · *Zingiber officinale* · Jejuna · Goblet cells · Mice

Introduction

Eimeria spp. are among the most destructive protozoans of the phylum Apicomplexa. *Eimeria* infection via fecal–oral transmission has mainly been associated with the disease coccidiosis. Interestingly, in cases of *Eimeria* infections, every part of the intestine has been observed to be infected with a specific *Eimeria* species (Lillehoj et al. 2015). The invasion of *Eimeria* sporozoites into the epithelial cells of the intestine of poultry animals results in diarrhea, malabsorption of nutrients leading to weight loss, and finally, death, thereby causing huge economic loss to the poultry industry (Alnassan et al. 2014). *Eimeria papillata* invades the jejunum of the mouse intestine (site of infection), leading to serious inflammation of the intestinal mucosa and increased oxidative conditions (Abdel-Latif et al. 2016). Therefore, this species is suitable for the evaluation of the impact of *Eimeria* infection in animal models (Dkhil 2013).

Responsible Editor: Philippe Garrigues.

✉ Felwa A. Thagfan
fathagfan@pnu.edu.sa

1 Department of Zoology and Entomology, Faculty of Science, Helwan University, Cairo, Egypt

2 Applied Science Research Center, Applied Science Private University, Amman, Jordan

3 Department of Biology, College of Science, Princess Nourah bint Abdulrahman University, Riyadh, Saudi Arabia

4 Department of Zoology, College of Science, King Saud University, Riyadh, Saudi Arabia

5 Department of Parasitology, Faculty of Veterinary Medicine, Alexandria University, Alexandria, Egypt

6 Department of Science Laboratories, College of Science and Arts, Qassim University, Ar-Rass 52719, Saudi Arabia

7 Clinical Laboratory Sciences Department, College of Applied Medical Sciences, King Saud University, Riyadh, Saudi Arabia

Nanotechnology is a promising research field having a variety of applications, especially in medicine and industry, (Zhao et al. 2017) with one of its most important applications being the control of a multitude of infectious diseases affecting animals and plants (Pimentel-Acosta et al. 2019; Resham et al. 2015). Silver nanoparticles (AgNPs) are considered to be efficient bactericidal, antifungal, and antiviral agents (Cho et al. 2018). In addition, AgNPs have good antiparasitic action against some protozoans infecting fishes like *Ichthyophthirius multifiliis* (Saleh et al. 2017). AgNPs can be synthesized by various chemical and physical methods that are known to be expensive, complex, and even involve toxic agents (Pimentel-Acosta et al. 2019). To overcome these issues, various techniques for the biosynthesis of AgNPs involving the use of different plants have been established as simple, eco-friendly, reliable, and inexpensive alternatives to chemical or physical methods (Bhakya et al. 2016).

The use of plant extracts enables NPs to be biosynthesized using specific plant parts instead of the whole plant. Extracts of various plants, such as aloe vera, ginger, honey, mango, amla, marigold, and lemon, have been reportedly used in the production and stabilization of NPs (Mehata 2021) *Zingiber officinale* rhizomes are widely used as a spice and for flavor in foods. They also have applications in the production of soaps, cosmetics, and more recently in medicine, such as in the treatment of coronavirus disease, stomach pain, cough, and in reducing the effect of acute chemotherapy-induced nausea in adult cancer patients (Ho et al. 2013; Semwal et al. 2015).

The present study aimed to evaluate the protective effect of AgNPs biosynthesized from *Z. officinale* on the jejunum in the intestines of mice infected with sporulated oocysts of *Eimeria papillata*.

Material and methods

Animals and parasite infection

Male mice (C57BL/6), aged 10–12 weeks, were used in this study. *E. papillata* oocysts were obtained from the feces of infected mice and were processed according to a method described in a previous study (Dkhil et al. 2011).

Preparation and phytochemical screening of *Zingiber officinale* extract

Z. officinale rhizomes were purchased from a market in Egypt. The plant specimens were validated by a taxonomist at the Department of Botany, Helwan University. The rhizomes were homogenized and subsequently used in the preparation of 70% *Z. officinale* methanolic extract (ZE) according to a method described by Thagfan et al. (2021).

The methanolic extract of ZE was subjected to gas chromatography–mass spectrometry analysis (GC–MS) using a Thermo Scientific™ Trace GC Ultra and ISQ™ Single Quadruple MS (Thermo Fisher Scientific, Waltham, USA) (Abdeen et al. 2019). Identification of the mass spectrum was conducted with reference to the Wiley Registry and National Institute Standard and Technology (NIST) databases.

Biosynthesis and characterization of silver nanoparticles

Briefly, AgNPs were biosynthesized by adding 45 mL of $AgNO_3$ (8×10^{-3} M, ~ 0.06793 g) solution to approximately 5 mL of freshly prepared ZE and placing the mixture in a black chamber. The formation of AgNPs in the solution was ensured by incubating it until the color changed from brownish to black.

The absorbance of AgNPs was monitored by measuring the ultraviolet (UV)-visible spectra at wavelengths ranging from 300 to 800 nm with a UV-1650 PC UV–visible spectrophotometer (Shimadzu, Osaka, Japan). The form and size of AgNPs were characterized by transmission electron microscopy (TEM) using a JEOL JEM-2100 (JEOL Ltd., Tokyo, Japan) according to a method described by Jiang et al. (2008). The AgNP structure was characterized by X-ray diffraction (XRD) analysis (XRD-6000; Shimadzu). The XRD patterns were recorded at a scan speed of 4°/min.

In vivo infection and experimental design

Each mouse was infected with 10^3 sporulated *E. papillata* oocysts by oral administration, and the number of oocysts per gram of feces was calculated. Thirty-two mice were divided into five groups of eight mice each. The first group, representing the negative control group, was administered distilled water. The second group was administrated 5 mg/kg AgNPs daily via oral gavage inoculations (Abd El Wahab et al. 2021). The third, fourth, and fifth groups were infected with 103 *E. papillata* oocysts inoculated via oral route (Dkhil et al. 2015). After one hour of infection, the fourth and fifth groups were treated with orally administered AgNPs and 25 mg/kg amprolium, respectively, for 5 days.

On day 5, oocyst shedding was quantified using a McMaster chamber and was expressed as the number of oocysts per gram of wet feces. Subsequently, all mice were euthanized, and portions of the jejunum were preserved in formalin to count the parasite stages and goblet cells.

Enumeration of parasites

To count the parasite stages, all mice were sacrificed, and the jejunum portions were preserved in formalin. The jejunum specimens were embedded in paraffin wax and fixed in 10% buffered formalin. Subsequently, 4-µm-thick sections prepared using a microtome were stained with hematoxylin and eosin (HE). Oocysts per ten microvilli were then counted by observation under a light microscope.

Histopathology and enumeration of goblet cells

The jejunum was removed, processed, fixed in neutral buffered formalin for 12 h, dehydrated, and embedded in paraffin. The sections were stained with HE. Histological injury score was assessed according to a method described by Dommels et al. (2007).

The sections were stained with Alcian blue to estimate the number of goblet cells. The average number of goblet cells in 20 villi was calculated for each animal.

Statistical analysis

The data were analyzed using a one-way ANOVA, and statistical comparisons between groups were performed using Duncan's test. Values are expressed as mean ± standard deviation (SD) at a significance level of $P \leq 0.05$.

Results

Results of GC–MS at different retention times are presented in Table 1 and Figure S1 showing the detection of 38 active phytochemical compounds. The major compounds identified in ZE were 1-(4-hydroxy-3-methoxyphenyl)tetradec-4-en3-one (4.1%), (3R,5S)-1-(4-hydroxy-3-methoxyphenyl)decane-3,5-diyl diacetate (4.6%), 4H-Pyran-4-one, 2,3-dihydro-3,5-dihydroxy-6-methyl- (5.9%), butan-2-one, 4-(3-hydroxy-2-methoxyphenyl)- (17.4%), 1-(4-hydroxy-3-methoxyphenyl)dec-4-en-3-one (18.4%), and butan-2-one, 4-(3-hydroxy-2-methoxyphenyl)- (29.3%).

TEM analysis showed that the size of the biosynthesized AgNPs was < 50 nm (Fig. 1). The formation of AgNPs was

Table 1 Effect of biosynthesized AgNPs on *E. papilata* developmental stages

Group	Number of meronts	Number of gamonts (males and females)	Number of oocysts inside the epithelium
Infected	158.3 ± 35	26.5 ± 1	7.4 ± 3
Infected + ZNPs	57.2 ± 10*	15.6 ± 2.8*	1.2 ± 0.8*
Infected + Amp	79.8 ± 9*	17.4 ± 5*	2.6 ± 1.1*

Data are mean ± SD in 10 villi. *,Significance against the infected group at $p \leq 0.05$

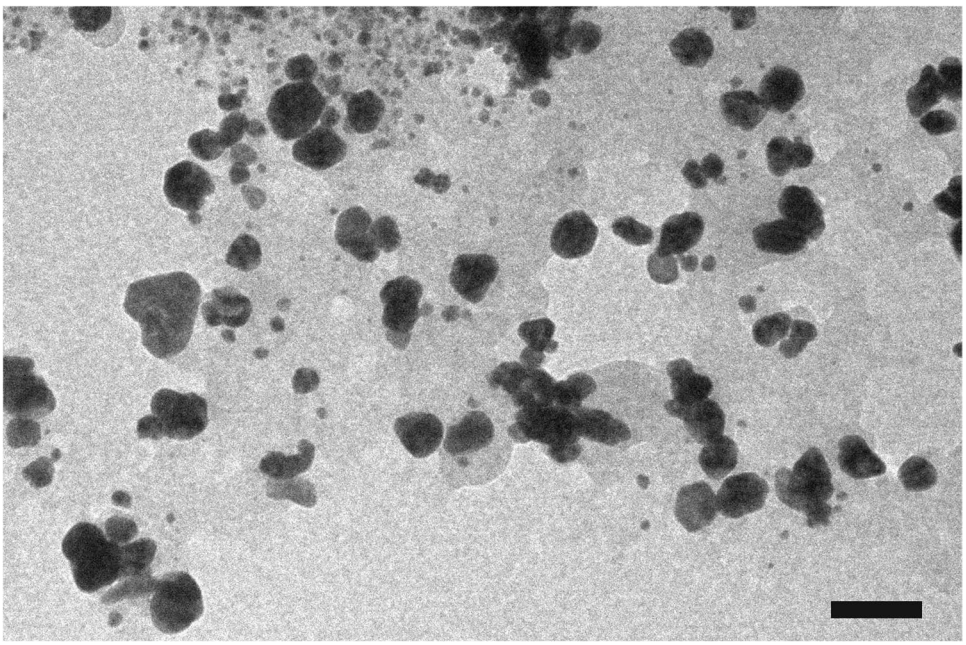

Fig. 1 TEM of AgNPs showing their size. Scale bar = 100 nm

confirmed by observing color change from yellow to dark brown on addition of ginger extract to the $AgNO_3$ solution. UV–visible spectroscopy for monitoring the production of AgNPs in the mixture revealed a strong and broad surface plasmon resonance peak at 450 nm, a characteristic feature of AgNPs (Fig. 2).

Figure 3 shows the XRD patterns of AgNPs. All particles had similar diffraction profiles and XRD at different peaks.

After five days, mice infected with sporulated *E. papillata* oocysts had an oocyst output of approximately 70×10^4 oocysts/g of feces. AgNP treatment of infected mice led to a significant decrease in the oocyst output compared to that of the untreated infected group and the amprolium-treated group (Fig. 4).

Histopathological changes were visible in the infected jejuna, particularly in the vacuolated injured jejunal mucosa, which contained lymphatic infiltration. In addition to observing the obvious destruction and shedding of jejunum epithelia caused by parasite invasion, the inflammatory status of the jejunum was assessed using a semi-quantitative scoring system. While the infected mice were reported to have mild inflammatory injury, AgNPs dramatically ameliorated the inflammatory lesions generated by *E. papillata* infection in mice (Fig. 5, Figure S2).

Analysis of the histological injury score showed inflammation in the jejunum of mice infected with *E. papillata*, and this inflammatory profile was significantly decreased after treatment with either AgNPs or amprolium (Fig. 6). Histological examinations of *E. papillata*-infected mice on day 5 post-infection showed a reduction in the number of goblet cells in comparison with that in the non-infected mice (Fig. 7). Treatment of infected mice with AgNPs significantly increased the number of goblet cells in the jejunal villi (Fig. 8).

The groups treated with AgNPs showed a significant decrease in the total number of parasitic stages in *E. papillata*-infected mice in comparison with that in the control group (Fig. 9). In addition, meronts, gamonts, and developed oocysts in the jejunum were significantly altered after treatment with AgNPs (Table 2).

Discussion

Since ancient times, plants or their parts have been used in the treatment of various diseases. The ginger (*Zingiber officinale*) plant, in addition to its role of flavoring food, has been commonly used for therapeutic purposes (Ghafoor et al. 2020). The therapeutic effect of ginger may be attributed to the bioactive compounds present in it. Our results showed that ZE contained many compounds having medicinal value, such as 1-(4-hydroxy-3-methoxyphenyl)tetradec-4-en3-one Butan-2-one, 4-(3-hydroxy-2-methoxyphenyl)-, which possesses antioxidant and antimicrobial activity (Hwang et al. 2013; Ghasemzadeh et al. 2018), Butan-2-one, 4-(3-hydroxy-2-methoxyphenyl)- which has antimicrobial activity (Ashraf et al. 2017), 1-(4-hydroxy-3-methoxyphenyl)dec-4-en-3-one, which induces apoptosis in human

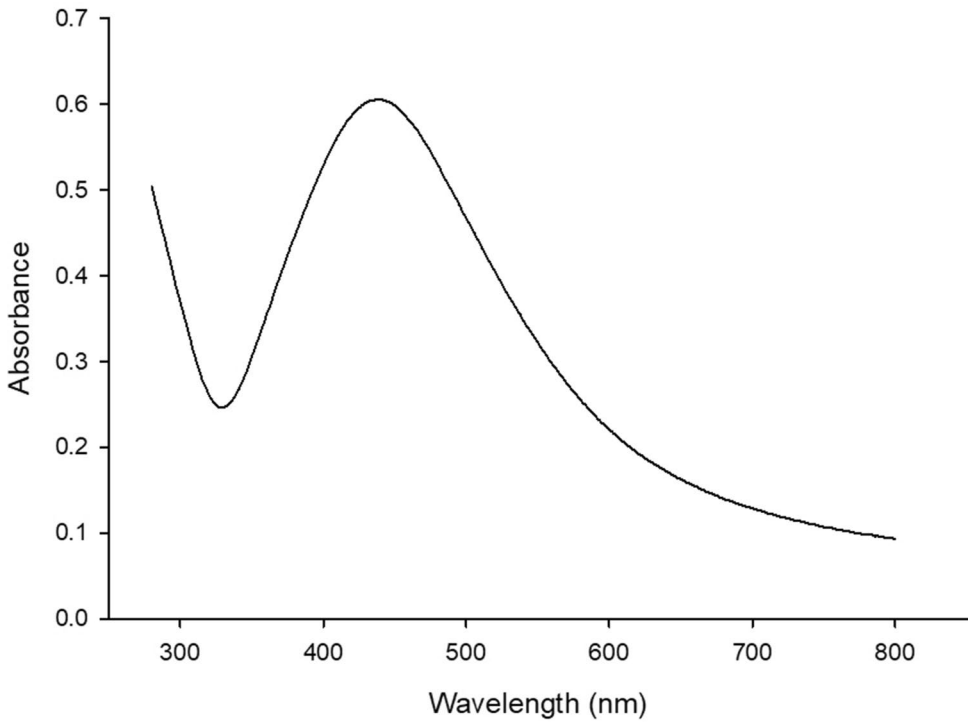

Fig. 2 UV–Visible absorption spectrum of the biosynthesized AgNPs

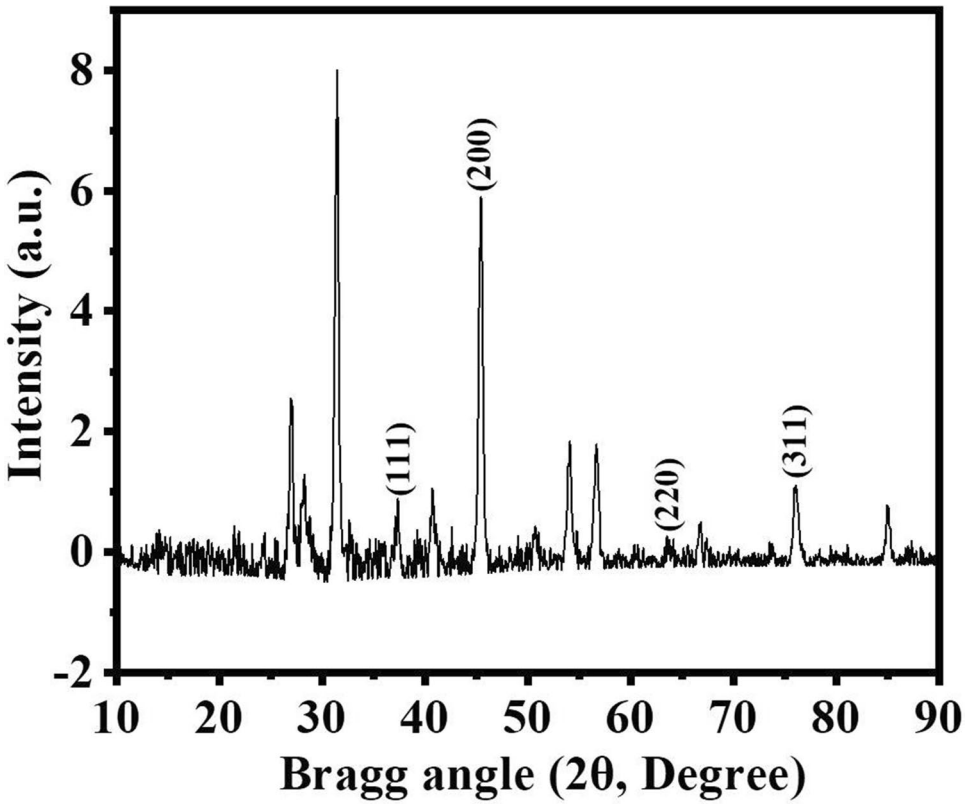

Fig. 3 X-ray diffraction pattern of biosynthesized AgNPs

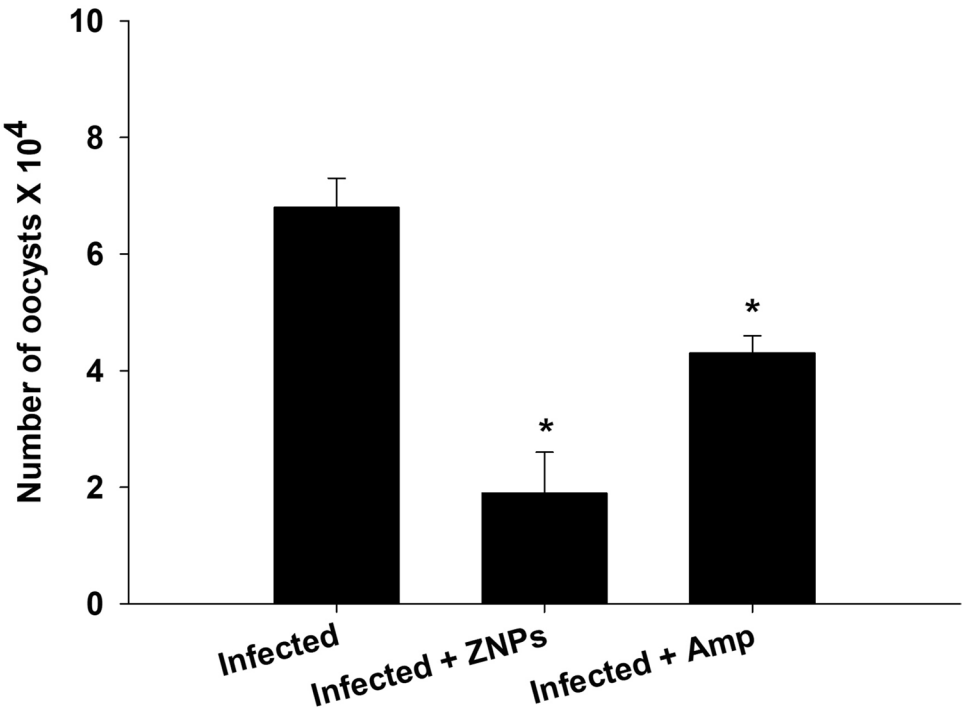

Fig. 4 Produced number of oocysts on day 5 postinfection. The values are represented as mean ± SD. *Significance against infected group at $P < 0.05$, $n = 8$

colorectal carcinoma cells via ROS production (Pan et al. 2008), and (3R,5S)-1-(4-hydroxy-3-methoxyphenyl)decane-3,5-diyl diacetate, which is reported to have extracellular melanogenesis inhibition activity (Yamauchi et al. 2019).

Ginger rhizomes are of medicinal importance as they contain bioactive compounds that have a wide range of applications in the pharmaceutical industry (Tomaino et al. 2005). Considering that toltrazuril, the currently used

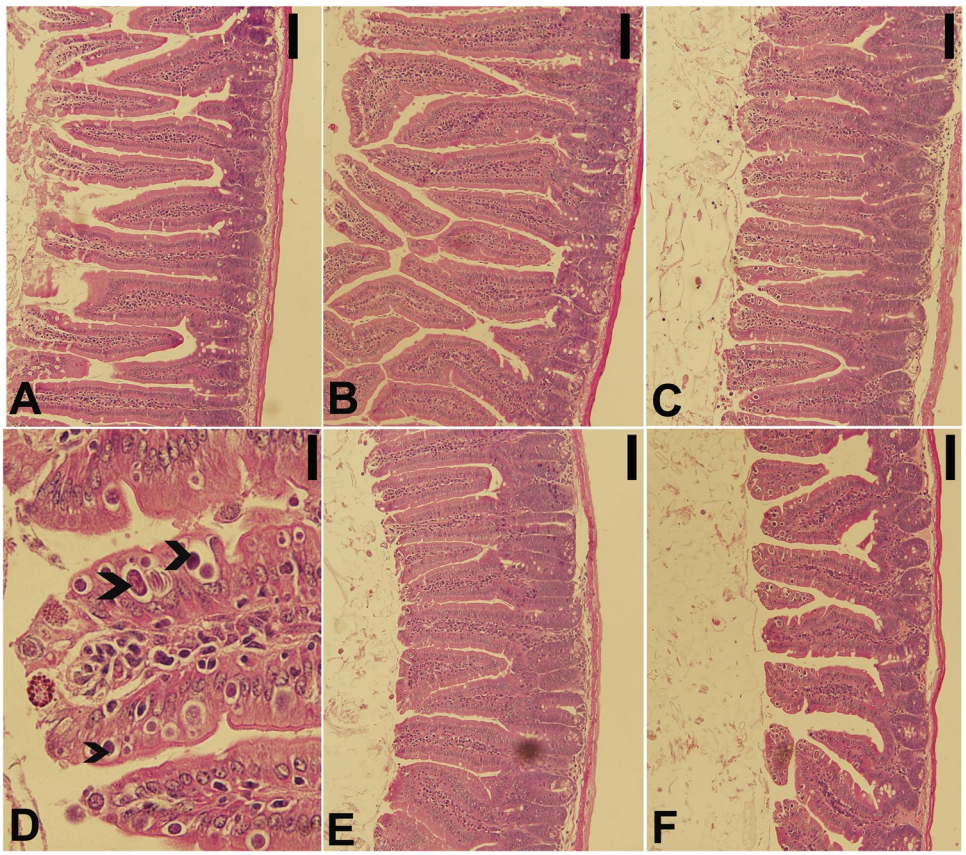

Fig. 5 Histological changes during infection and after treatment with AgNPs. (**A**) Non-infected jejunum. (**B**) AgNP-treated jejunum. (**C, D**) Infected jejunum. Arrow head for parasitic stages of *E. papillata*. (**E**) Infected-treated jejunum treated with AgNPs. (**F**) Infected-treated Jejunum treated with Amp. Sections stained with H&E. Scale bar = 100 µm for **A**, **B**, **C**, **E**, and **F**. For **D**, the scale bar = 25 µm. $N = 5$

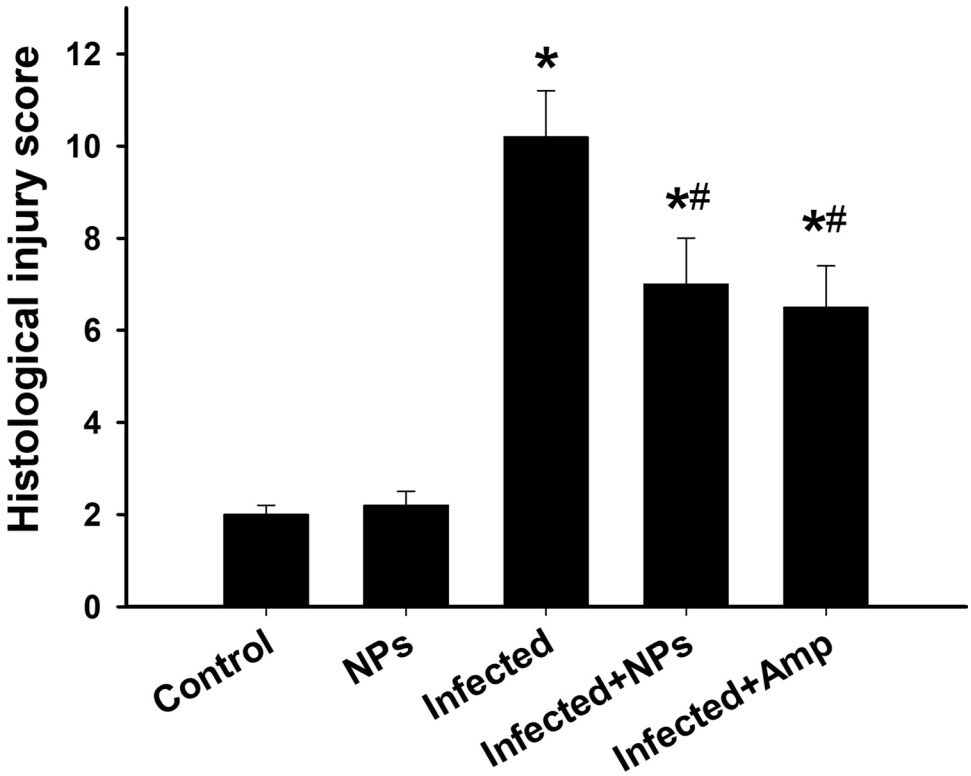

Fig. 6 The score of histological injury of the noninfected and *Eimeria papillata*-infected and *Eimeria papillata*-treated groups. The values are represented as mean ± SD. Significance against non-infected (*) and infected (#) group at $P < 0.05$

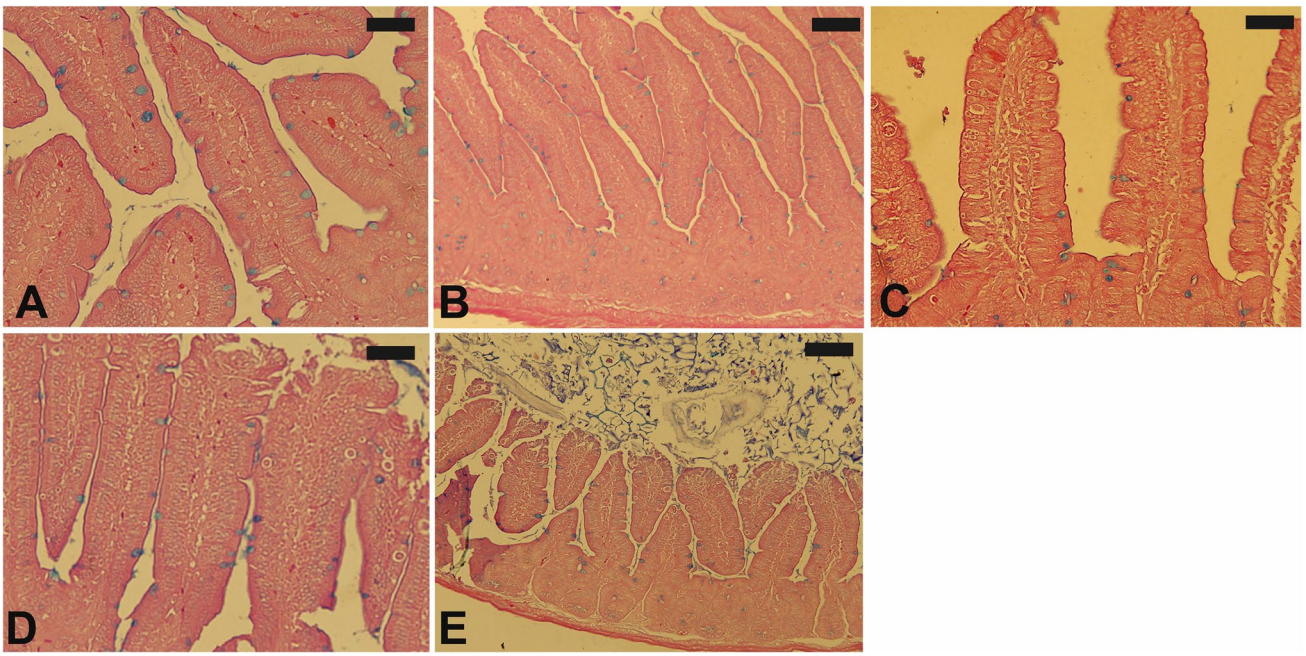

Fig. 7 Goblet cells in the jejunum stained with Alcian blue, (**A**) control group, (**B**) AgNPs, and (**C**) infected group, while (**D**) and (**E**) are the treated groups with AgNPs and Amp, respectively. $N = 5$. Scale bar = 50 µm

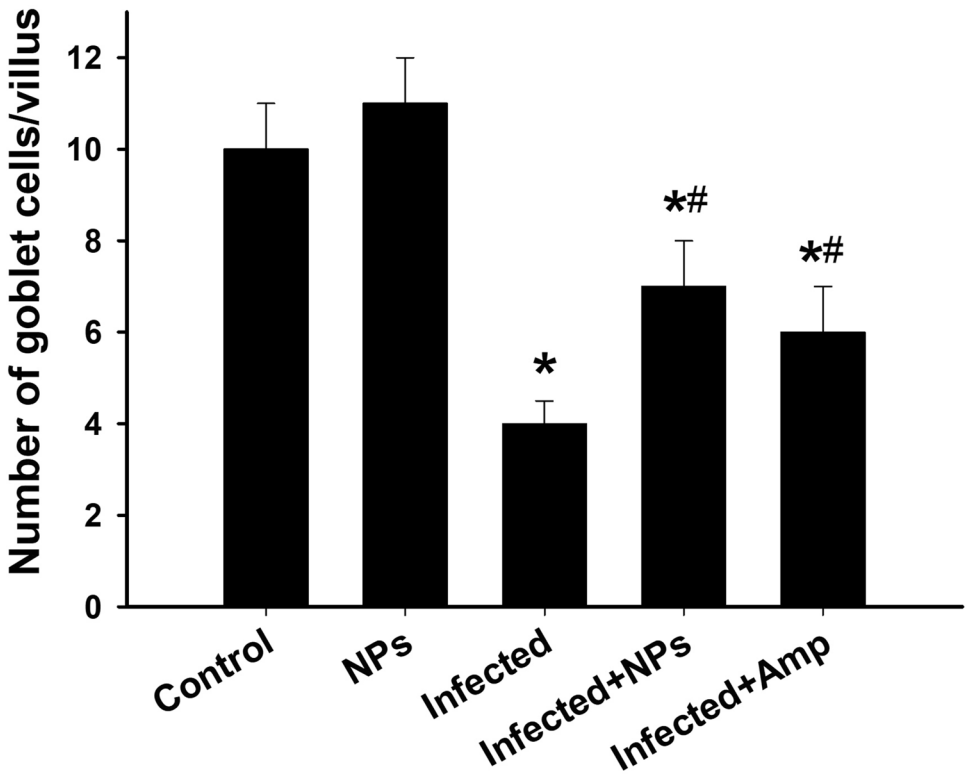

Fig. 8 The effect of treated mice with AgNPs or Amp on the number of jejunal goblet cells. $N = 5$. The values are represented as mean ± SD. Significance against non-infected (*) and infected (#) group at $P < 0.05$

anticoccidial drug for eimeriosis (Alnassan et al. 2013), has side effects in animal tissues and/or in their products, such as eggs, (Dkhil et al. 2015); we prepared AgNPs from ginger rhizomes as a green eco-friendly alternative.

AgNPs showed an anticoccidial effect in the *E. papillata*-infected mice, which was confirmed in terms of an observed reduction of oocyst count in the feces of treated mice in comparison with that in control mice.

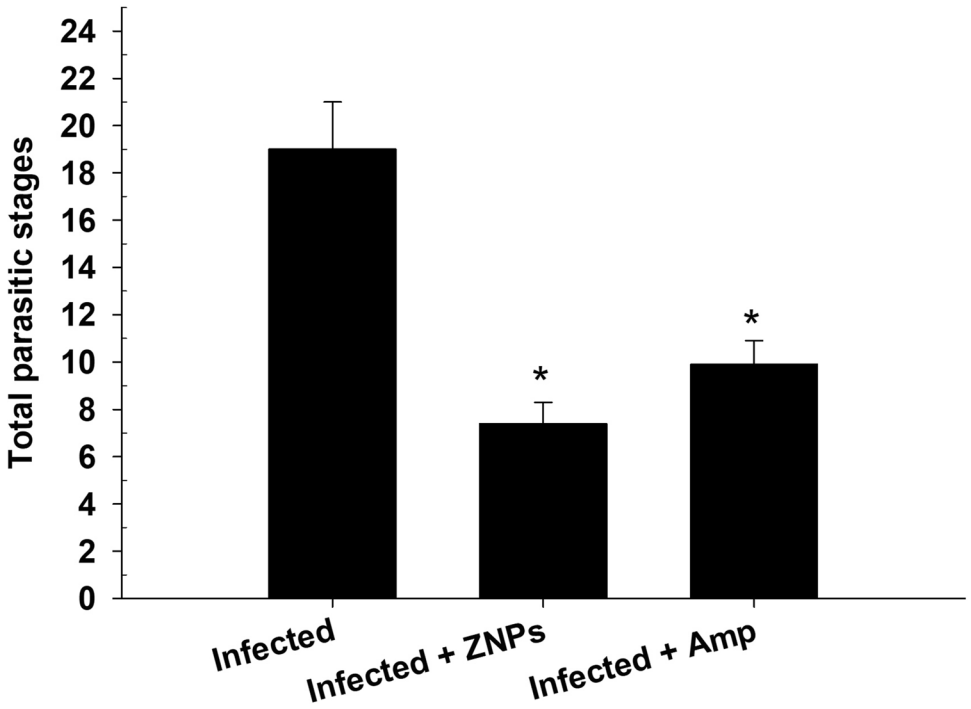

Fig. 9 Effect of treatment of *E. papillata*-infected mice with AgNPs and Amp. on the parasitic stages counting in 10 VCU/mouse. The values are represented as mean ± SD. Significance against non-infected (*) and infected (#) group at $P < 0.05$

Abdel-Latif et al. (2016) have reported that chitosan activity leads to reduction in the number of oocysts in the feces of *E. papillata*-infected mice. These observations are also in agreement with results reported by Dkhil et al. (2015) showing berberine to have a similar effect in treating *Eimeria* infections in mice. In the present study, the treatment of *E. papillata*-infected mice with biosynthesized AgNPs was shown to reduce the duplication and intracellular development of *E. papillata* in the jejunal epithelial cells of mice. This action of AgNPs can be considered to contribute to their anti-inflammatory and antioxidant effects.

In the present study, histopathological examination of the jejuna of *E. papillata*-infected mice showed many lesions, vacuolations of the epithelium, and destruction of certain villi. After treatment with biosynthesized AgNPs, histological changes were significantly improved in the jejuna of the infected mice. Thagfan et al. (2021) found similar ameliorative effects of *Morus nigra* leaf extracts on the histology of the jejunal epithelium of *E. papillata*-infected mice. Thagfan et al. (2021) and Alkhudhayri et al. (2018) reported a similar improvement of histopathological changes in the jejunum of *E. papillata*-infected mice on treatment with selenium nanoparticles.

Goblet cells found in the intestine secrete mucus that acts as an immune-defensive barrier against microbes and parasites that may invade the intestine during food ingestion (Parmar et al. 2021). Many studies have reported that goblet cells are highly affected by *Eimeria* infection (Dkhil et al. 2013; Kim et al. 1996) In the current study, histological sections of jejuna of *E. papillata*-infected mice observed on day 5 postinfection showed a reduction in the number of goblet cells (Figs. 7 and 8). Treatment with biosynthesized AgNPs increased the number of goblet cells in the jejuna. In agreement with the results of the present study, the studies by Abdel-Latif et al. (2016) and Alkhudhayri et al. (2018) mentioned previously also report an increase in the number of goblet cells by the action of chitosan and selenium nanoparticles, respectively, in *E. papillata*-infected mice. Cheng and Leblond (1974) suggested that parasite infection may impair the stem cells found in intestinal crypts that produce goblet cells and this phenomenon could be considered as the reason for the reduction in the number of goblet cells. Interestingly, Alkhudhayri et al. (2018) reported upregulation of the goblet cell-specific gene *Muc2* in mice treated with selenium nanoparticles.

Conclusion

This study showed biosynthesized AgNPs to be effective against *E. papillata* infection in mice. The action of biosynthesized AgNPs was shown to reduce the invasion of *E. papillata* in the jejunal epithelia and result in enhanced killing of *E. papillata* at different stages, which was confirmed in terms of low oocyst output in feces of infected mice. More studies are required to cover all aspects of biosynthesized AgNP treatment of infected mice, including analysis of ultrastructural changes in the jejunal epithelia, oxidative stress, and other effects at the molecular level. Moreover, future research should also focus on molecular analysis to identify the genes that are controlled during infection.

Table 2 Identification of phytochemical compounds by GC-Mass in *Zingiber officinale* extract

Component RT	Compound name	Molecular weight	[M-H]- (m/z) molecular weight-1	Formula	Area	Peak %
1.1303	Dimethylamine	45.0837	44.0837	C_2H_7N	228,135,067	1.047661706
1.6259	Carbonic acid, ethyl 2-propenyl ester	130.1418	129.1418	$C_6H_{10}O_3$	11,332,076	0.052040145
2.3007	Hexanal	100.1589	99.1589	$C_6H_{12}O$	126,339,131	0.580185551
2.5612	Acetic acid	60.0520	59.052	$C_2H_4O_2$	313,764,424	1.440896291
3.3843	Cyclooctyl alcohol	128.2120	127.212	$C_8H_{16}O$	231,692,987	1.064000696
3.8265	3-Benzoyl-5-[2-(phenylthio)ethyl]-3,4- diazatricyclo[5.2.1.0(2,6)]dec-4-ene	376.5	375.5	$C_{23}H_{24}N_2OS$	141,037,231	0.647683445
4.1020	4H-Pyran-4-one, 2,3-dihydro-3,5-dihydroxy-6- methyl-	144.1253	143.1253	$C_6H_8O_4$	1,288,212,662	5.915842284
4.7163	Iso-Amyl tiglate	170.2487	169.2487	$C_{10}H_{18}O_2$	473,929,136	2.176418619
5.0353	Eugenol	164.2011	163.2011	$C_{10}H_{12}O_2$	144,068,476	0.661603792
5.9356	2,4-Di-tert-butylphenol	206.3239	205.3239	$C_{14}H_{22}O$	258,344,144	1.186390459
6.3324	(1S,2E,6E,10R)-3,7,11,11- Tetramethylbicyclo[8.1.0]undeca-2,6-diene	204.3511	203.3511	$C_{15}H_{24}$	162,634,245	0.746863132
6.7993	Pipecolic acid, N-ethoxycarbonyl-, octyl ester	313.4	312.4	$C_{17}H_{31}NO_4$	551,771,665	2.533893854
7.1129	Butan-2-one, 4-(3-hydroxy-2-methoxyphenyl)-	194.2271	193.2271	$C_{11}H_{14}O_3$	3,793,915,802	17.42275028
7.4459	4-(2,4-Dimethoxyphenyl)butan-2-one	208.254	207.254	$C_{12}H_{16}O_3$	265,489,450	1.219203755
7.9909	Phenol, 5-(1,5-dimethyl-4-hexenyl)-2-methyl-, (R)-	218.3346	217.3346	$C_{15}H_{22}O$	43,033,343	0.197621462
8.3357	Benzene, 1-(1,1-dimethylethyl)-3,5-dimethyl-	162.2713	161.2713	$C_{12}H_{18}$	10,947,730	0.050275118
8.6704	3-Buten-2-one, 4-(4-hydroxy-3- methoxyphenyl)-	192.2112	191.2112	$C_{11}H_{12}O_3$	149,937,296	0.688555098
9.0728	Hexanedioic acid, mono(2-ethylhexyl)ester	258.35	257.35	$C_{14}H_{26}O_4$	156,441,793	0.718425615
9.6852	Hexadecanoic acid, methyl ester	270.4507	269.4507	$C_{17}H_{34}O_2$	26,553,501	0.121941298
10.0130	n-Hexadecanoic acid	256.4241	255.4241	$C_{16}H_{32}O_2$	52,125,672	0.239376047
10.5018	4-Morpholineacetonitrile,.alpha.-phenethylidene-	228.290	227.29	$C_{14}H_{16}N_2O$	17,881,140	0.082115327
10.8850	(E)-1-(6,10-Dimethylundec-5-en-2-yl)-4-methylbenzene	272.47	271.47	$C_{20}H_{32}$	25,346,936	0.116400405
11.4534	1-(4-Hydroxy-3-methoxyphenyl)oct-4-en-3-one	248.3175	247.3175	$C_{15}H_{20}O_3$	37,056,022	0.170171889
12.4495	2-Butanone, 4-(4-hydroxy-3-methoxyphenyl)-	194.2271	193.2271	$C_{11}H_{14}O_3$	134,101,729	0.615833629
12.9815	3-Decanone, 1-(4-hydroxy-3-methoxyphenyl)-	278.3865	277.3865	$C_{17}H_{26}O_3$	337,285,165	1.548910284

Table 2 (continued)

Component RT	Compound name	Molecular weight	[M-H]- (m/z) molecular weight-1	Formula	Area	Peak %
13.5979	1-(4-Hydroxy-3-methoxyphenyl)dec-4-en-3-one	276.3707	275.3707	$C_{17}H_{24}O_3$	4,020,860,357	18.46494482
13.9098	1-(4-Hydroxy-3-methoxyphenyl)decane-3,5-dione	292.4	291.4	$C_{17}H_{24}O_4$	106,745,446	0.490205726
14.2833	Butan-2-one, 4-(3-hydroxy-2-methoxyphenyl)-	194.2271	193.2271	$C_{11}H_{14}O_3$	6,399,413,510	29.38794358
14.9799	(3R,5S)-1-(4-Hydroxy-3-methoxyphenyl) decane-3,5-diyl diacetate	380.4752	379.4752	$C_{21}H_{32}O_6$	1,021,953,670	4.693104571
15.4564	5-Hydroxy-1-(4-hydroxy-3-methoxyphenyl) dodecan-3-one	322.4	321.4	$C_{19}H_{30}O_4$	178,446,849	0.819479148
16.1382	1-(4-Hydroxy-3-methoxyphenyl)tetradec-4-en3-one	332.5	331.5	$C_{21}H_{32}O_3$	894,238,903	4.106601705
16.4355	1-(4-Hydroxy-3-methoxyphenyl)tetradecane-3,5-dione	348.5	347.5	$C_{21}H_{32}O_4$	97,502,585	0.447759855
16.9058	2-Butanone, 4-(4-hydroxy-3-methoxyphenyl)-	194.2271	193.2271	$C_{11}H_{14}O_3$	13,262,060	0.060903186
17.4487	4(1H)-Quinolone, 2,3-dihydro-6-methoxy-2- methyl-1-(p-tolylsulfonyl)-	345.4	344.4	$C_{18}H_{19}NO_4S$	6,243,408	0.028671522
17.8666	Caprolactone oxime, (NB)-O- [(diethylboryloxy)(ethyl)boryl]-			C12H25B2NO2	37,389,839	0.171704872
18.5173	Alanine, N-methyl-N-(2-chloroethoxycarbonyl)-, pentadecyl ester	420.0	419	$C_{22}H_{42}ClNO_4$	16,385,364	0.075246294
19.1360	2-Hydroxy-6-methyl-2-trifluoromethyl-4Hbenzo[1,4]oxazin-3-one	247.17	246.17	$C_{10}H_8F_3NO_3$	1,467,144	0.006737546
19.7918	Diundecylneopentylamine	395.7	394.7	$C_{27}H_{57}N$	356,465	0.00163699

Supplementary Information The online version contains supplementary material available at https://doi.org/10.1007/s11356-023-25383-0.

Author contribution Infection and treatment of animals were performed by M.A.D., E.M.A, F.A.T, A.A.B., and S.E. Biochemical, parasitological, and histological methodology and investigation were carried out by M.A.D., F.A.T., R.A., M.M., M.Y.M., and T.H. Data analysis, software, data curation, and visualization were performed by S.A., F.A.T., R.A., and E.M.A. Writing—reviewing and editing manuscript was performed by M.A.D., R.A., F.A.T., S.A., and M.Y.M. All authors participated in the design and interpretation of the study and approved the final manuscript.

Funding This study was supported by the Princess Nourah bint Abdulrahman University Researchers Supporting Project number (PNURSP2023R96), Princess Nourah bint Abdulrahman University, Riyadh, Saudi Arabia, and also was supported by Researchers Supporting Project (RSP2023R25), King Saud University, Riyadh, Saudi Arabia.

Data availability All relevant data are within the paper.

Declarations

Ethical approval The experiments were approved (approval no. HU2021/Z/AD/1213–2) by the Committee of Research Ethics for Laboratory Animal Care of the Department of Zoology, Faculty of Science, Helwan University.

Consent to participate This is not applicable.

Consent for publication The authors consented.

Conflict of interest The authors declare no competing interests.

References

Abd El Wahab WM, El-Badry AA, Mahmoud SS, El-Badry YA, El-Badry MA, Hamdy DA (2021) Ginger (Zingiber Officinale)-derived nanoparticles in Schistosoma mansoni infected mice: Hepatoprotective and enhancer of etiological treatment. PLoS Negl Trop Dis 15:e0009423

Abdeen A, Abdelkader A, Abdo M, Wareth G, Aboubakr M, Aleya L, Abdel-Daim M (2019) Protective effect of cinnamon against acetaminophen-mediated cellular damage and apoptosis in renal tissue. Environ Sci Pollut Res 26:240–249

Abdel-Latif M, Abdel-Haleem HM, Abdel-Baki A-AS (2016) Anticoccidial activities of chitosan on Eimeria papillata-infected mice. Parasitol Res 115:2845–2852

Alkhudhayri AA, Dkhil MA, Al-Quraishy S (2018) Nanoselenium prevents eimeriosis-induced inflammation and regulates mucin gene expression in mice jejunum. Int J Nanomed 13:1993

Alnassan A, Kotsch M, Shehata A, Krüger M, Daugschies A, Bangoura B (2014) Necrotic enteritis in chickens: development of a straightforward disease model system. Veterinary Record 174:555–555

Alnassan AA, Shehata AA, Kotsch M, Schrödl W, Krüger M, Daugschies A, Bangoura B (2013) Efficacy of early treatment with toltrazuril in prevention of coccidiosis and necrotic enteritis in chickens. Avian Pathol 42:482–490

Ashraf SA, Al-Shammari E, Hussain T, Tajuddin S, Panda BP (2017) In-vitro antimicrobial activity and identification of bioactive components using GC–MS of commercially available essential oils in Saudi Arabia. J Food Sci Technol 54:3948–3958

Bhakya S, Muthukrishnan S, Sukumaran M, Grijalva M, Cumbal L, Benjamin JF, Kumar TS, Rao M (2016) Antimicrobial, antioxidant and anticancer activity of biogenic silver nanoparticles–an experimental report. RSC Adv 6:81436–81446

Cheng H, Leblond C (1974) Origin, differentiation and renewal of the four main epithelial cell types in the mouse small intestine V. Unitarian theory of the origin of the four epithelial cell types. Am J An 141:537–561

Cho Y-M, Mizuta Y, Akagi J-i, Toyoda T, Sone M, Ogawa K (2018) Size-dependent acute toxicity of silver nanoparticles in mice. J Toxicol Pathol 31:73–80

Dkhil MA, Moniem AEA, Al-Quraishy S, Saleh RA (2011) Antioxidant effect of purslane (Portulaca oleracea) and its mechanism of action. J Med Plants Res 5:1589–1593

Dkhil MA (2013) Anti-coccidial, anthelmintic and antioxidant activities of pomegranate (Punica granatum) peel extract. Parasitol Res 112:2639–2646

Dkhil MA, Al-Quraishy S, Moneim AEA, Delic D (2013) Protective effect of Azadirachta indica extract against Eimeria papillata-induced coccidiosis. Parasitol Res 112:101–106

Dkhil MA, Metwaly MS, Al-Quraishy S, Sherif NE, Delic D, Al Omar SY, Wunderlich F (2015) Anti-Eimeria activity of berberine and identification of associated gene expression changes in the mouse jejunum infected with Eimeria papillata. Parasitol Res 114:1581–1593

Dommels Y, Butts C, Zhu S, Davy M, Martell S, Hedderley D, Barnett M, McNabb W, Roy N (2007) Characterization of intestinal inflammation and identification of related gene expression changes in mdr1a−/− mice. Genes Nutr 2:209–223

Ghafoor K, Al Juhaimi F, Özcan MM, Uslu N, Babiker EE, Ahmed IAM (2020) Total phenolics, total carotenoids, individual phenolics and antioxidant activity of ginger (Zingiber officinale) rhizome as affected by drying methods. Lwt 126:109354

Ghasemzadeh A, Jaafar HZ, Baghdadi A, Tayebi-Meigooni A (2018) Formation of 6-, 8-and 10-shogaol in ginger through application of different drying methods: altered antioxidant and antimicrobial activity. Molecules 23:1646

Ho S-C, Chang K-S, Lin C-C (2013) Anti-neuroinflammatory capacity of fresh ginger is attributed mainly to 10-gingerol. Food Chem 141:3183–3191

Hwang IG, Kim HY, Woo KS, Lee SH, Lee J, Jeong HS (2013) Isolation and identification of the antioxidant DDMP from heated pear (Pyrus pyrifolia Nakai). Prevent Nutri Food Sci 18:76

Jiang J, Oberdörster G, Elder A, Gelein R, Mercer P, Biswas P (2008) Does nanoparticle activity depend upon size and crystal phase? Nanotoxicology 2:33–42

Kim YS, Gum J, Brockhausen I (1996) Mucin glycoproteins in neoplasia. Glycoconjugate J 13:693–707

Lillehoj H, Jang S, Lee S, Lillehoj E (2015): Chapter 4: Avian coccidiosis as a prototype intestinal disease—host protective immunity and novel disease control strategies, Intestinal health: Key to maximise growth performance in livestock. Wageningen Academic Publishers, pp. 79

Mehata MS (2021) Green route synthesis of silver nanoparticles using plants/ginger extracts with enhanced surface plasmon resonance and degradation of textile dye. Mater Sci Eng, B 273:115418

Pan MH, Hsieh MC, Kuo JM, Lai CS, Wu H, Sang S, Ho CT (2008) 6-Shogaol induces apoptosis in human colorectal carcinoma cells via ROS production, caspase activation, and GADD 153 expression. Mol Nutr Food Res 52:527–537

Parmar N, Burrows K, Vornewald PM, Lindholm HT, Zwiggelaar RT, Díez-Sánchez A, Martín-Alonso M, Fosslie M, Vallance BA, Dahl JA (2021) Intestinal-epithelial LSD1 controls goblet cell maturation and effector responses required for gut immunity to bacterial and helminth infection. PLoS Pathog 17:e1009476

Pimentel-Acosta CA, Morales-Serna FN, Chávez-Sánchez MC, Lara HH, Pestryakov A, Bogdanchikova N, Fajer-Ávila EJ (2019) Efficacy of silver nanoparticles against the adults and eggs of monogenean parasites of fish. Parasitol Res 118:1741–1749

Resham S, Khalid M, Kazi AG (2015): Nanobiotechnology in agricultural development, PlantOmics: the omics of plant science. Springer, pp. 683–698

Saleh M, Abdel-Baki A-A, Dkhil MA, El-Matbouli M, Al-Quraishy S (2017) Antiprotozoal effects of metal nanoparticles against Ichthyophthirius multifiliis. Parasitology 144:1802–1810

Semwal RB, Semwal DK, Combrinck S, Viljoen AM (2015) Gingerols and shogaols: important nutraceutical principles from ginger. Phytochemistry 117:554–568

Thagfan FA, Al-Megrin WA, Al-Shaebi EM, Al-Quraishy S, Dkhil MA (2021) Protective role of Morus nigra leaf extracts against murine infection with Eimeria papillata. Comb Chem High Throughput Screening 24:1603–1608

Tomaino A, Cimino F, Zimbalatti V, Venuti V, Sulfaro V, De Pasquale A, Saija A (2005) Influence of heating on antioxidant activity and the chemical composition of some spice essential oils. Food Chem 89:549–554

Yamauchi K, Natsume M, Yamaguchi K, Batubara I, Mitsunaga T (2019) Structure-activity relationship for vanilloid compounds from extract of Zingiber officinale var rubrum rhizomes: effect on extracellular melanogenesis inhibitory activity. Med Chem Res 28:1402–1412

Zhao K, Li S, Li W, Yu L, Duan X, Han J, Wang X, Jin Z (2017) Quaternized chitosan nanoparticles loaded with the combined attenuated live vaccine against Newcastle disease and infectious bronchitis elicit immune response in chicken after intranasal administration. Drug Delivery 24:1574–1586